UC San Diego
UC San Diego Previously Published Works

Title
Improvement of time-reversal communications using adaptive channel equalizers

Permalink
https://escholarship.org/uc/item/3bj5w52n

Journal
IEEE Journal of Oceanic Engineering, 31(2)

ISSN
0364-9059

Authors
Song, Hee C
Hodgkiss, W S
Kuperman, W A
et al.

Publication Date
2006-04-01

Peer reviewed

Improvement of Time-Reversal Communications Using Adaptive Channel Equalizers

H. C. Song, W. S. Hodgkiss, *Member, IEEE*, W. A. Kuperman, M. Stevenson, and T. Akal

Abstract—The spatial and temporal focusing properties of time-reversal methods can be exploited for undersea acoustic communications. Spatial focusing mitigates channel fading and produces a high signal-to-noise ratio (SNR) at the intended receivers along with a low probability of interception elsewhere. While temporal focusing (compression) reduces significantly intersymbol interference (ISI), there always is some residual ISI depending upon the number of transmitters, their spatial distribution (spatial diversity), and the complexity of the channel. Moreover, a slight change in the environment over the two-way propagation interval introduces additional ISI. Using multilevel quadrature amplitude modulation (M-QAM) in shallow water, we demonstrate that the performance of time-reversal communications can be improved significantly by cascading the received time series with an adaptive channel equalizer to remove the residual ISI.

Index Terms—Adaptive equalizer, billboard array, decision-feedback equalizer (DFE), decision-feedback phase-locked loop (DFPLL), fractionally spaced equalizer (FSE), intersymbol interference (ISI), multilevel quadrature amplitude modulation (M-QAM), multiple-input–multiple-output (MIMO), time-reversal communication.

I. INTRODUCTION

THE bandwidth-limited underwater acoustic (UWA) channel is a challenging environment for reliable coherent communications [1]. The UWA channel characterized by a time-varying, dispersive, multipath environment suffers from intersymbol interference (ISI) which causes severe distortion on the communication signals and results in performance degradation in high data rate systems. Multichannel adaptive channel equalizers [2] have been developed to cope with the ISI coupled with temporal variations in the undersea environment.

Recently, a relatively simple time-reversal approach has been introduced to underwater communications motivated by advances in time-reversal theory [3], [4] which involves multiple transmit/receive transducers referred to as a time-reversal mirror (TRM). The spatial and temporal focusing capability of the TRM offers a potential application to the communications problem especially in an environment with significant multipath. An initial system concept has been demonstrated using experimental data collected in shallow water for both active [5] and passive [6] time-reversal communications. The TRM is equivalent to a base station with multiple transmit/receive antennas in wireless communication and active and passive communications correspond to the downlink (from the base station to a user) and the uplink (from a user to the base station), respectively. Most recently, time-reversal communications have been extended to multiple-input–multiple-output (MIMO) multiuser communications such that different messages were sent simultaneously from a TRM (base station) to different receivers (users) at 8.6-km range in 105-m-deep shallow water [7]. It also has been demonstrated recently in wireless communications based on outdoor measurements that the use of time reversal (TR) has a promising potential in mitigating the ISI and in reducing the cochannel interference [8]. The benefit of the time-reversal approach is a simple receiver structure (lower complexity) as opposed to the high computational complexity required in adaptive channel equalizers.

Although the temporal focusing (compression) achieved by the time-reversal approach reduces ISI significantly, there always is some residual ISI depending upon the number of transmitters, the complexity of the channel, and their spatial distribution (diversity). Moreover, a slight change in the environment over the two-way propagation interval introduces additional ISI. The impact of residual ISI will be more crucial in higher order constellations required for higher data rate in a band-limited UWA channel. One obvious choice for mitigating the residual ISI would be to reduce the data rate (i.e., rate backoff).

In this paper, we investigate the time-reversal approach combined with adaptive channel equalization to enhance the performance of time-reversal communication without compromising the data rate. In fact, Stojanovic [9] demonstrated using analytical expressions for theoretical upper bounds that the performance of TR with residual ISI saturates as opposed to the performance of TR with equalization in terms of the output signal-to-noise ratio (SNR). We will show that the combination actually provides nearly optimal performance by re-examining the example used in [9]. The benefit of this combination is that the number of taps required for an equalizer is much smaller than the case with just an equalizer alone, thereby resulting in lower computational complexity at the equalizer. In this approach, phase tracking will be carried out at the front end of the optimal receiver before the equalizer.

This paper will present experimental results of coherent time-reversal communications at 3.5 kHz with a 1-kHz band-

H. C. Song, W. S. Hodgkiss, and W. A. Kuperman are with the Marine Physical Laboratory (MPL), Scripps Institution of Oceanography, La Jolla, CA 92093-0238 USA (e-mail: hcsong@mpl.ucsd.edu; wsh@mpl.ucsd.edu; wak@mpl.ucsd.edu).

M. Stevenson is with NATO Undersea Research Center, La Spezia 19138, Italy (e-mail: jms@saclantc.nato.int).

T. Akal was with NATO Undersea Research Centre, La Spezia, Italy. He is now with the Marine Physical Laboratory (MPL), Scripps Institution of Oceanography, La Jolla, CA 92093-0238 USA, and also with TUBITAK-MAN, Marmara Research Center, Earth and Marine Science Research Institute, Kocaeli 41470, Turkey (e-mail: tuakal@yahoo.com).
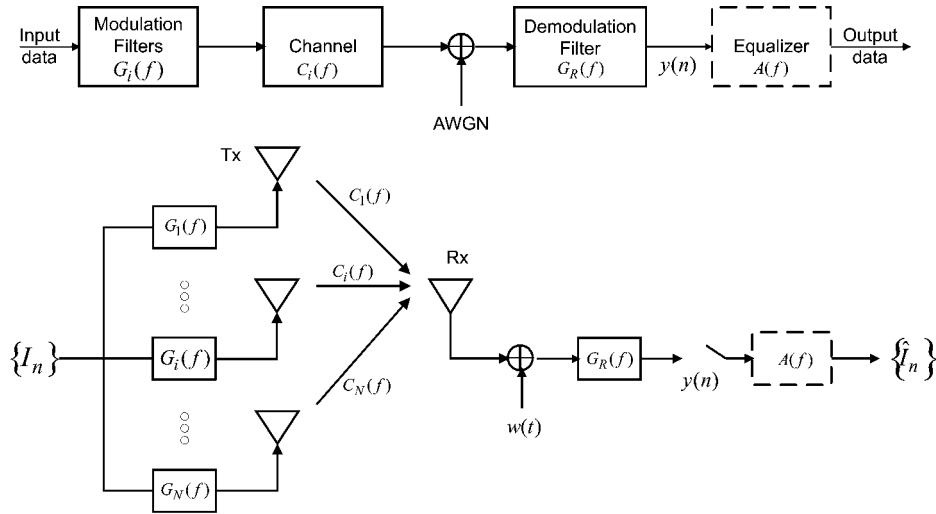
Fig. 1.   System model for active (downlink) time-reversal communications followed by a linear equalizer (dashed box).

width using high-order constellations (8-PSK, 16-QAM, and 32-QAM) during the Focused Acoustic Fields 2004 (FAF-04) experiment. The theory behind time-reversal communication is discussed briefly in Section II. Section III reviews the performance of time-reversal communication combined with a linear equalizer described in [9], followed by experimental results in Section IV.

II. TR COMMUNICATIONS

The theory behind the use of TR in an acoustic communications context has been presented in our previous paper [5]. Two-way TR can be seen as implementing actively a spatiotemporal matched filter of the impulse response (Green's function) of the waveguide from a signal processing point of view. However, TR also is based on waveguide physics which exploits the complexity of the environment using a time-reversal array for diversity gain [3]. When a known signal $s(t)$ is transmitted from a probe source (PS) in a waveguide, the (noiseless) received signal on the ith element of the TR array is $r_i(t) = s(t) * c_i(t)$ where $c_i(t)$ is the channel impulse response of the waveguide and $*$ denotes convolution. The N-element time-reversal array then retransmits the time reversed version of the received signal $r_i(-t)$. The signal received back at the original PS position $s_{\mathrm{ps}}(t)$ can be written as

$$
\begin{aligned}
s_{\mathrm{ps}}(t) &= s(-t) * \left[\sum_{i=1}^{N} c_i(t) * c_i(-t) \right] \\
&= s(-t) * q(t)
\end{aligned}
\tag{1}
$$

where the term in the bracket is denoted here by q-function (instead of Q-function in [10]) and is the summation of the autocorrelation of each channel impulse response. The performance of the TR focus depends on the complexity of the channel $c_i(t)$ (i.e., the number of multipaths), the number of TRM elements N, and their spatial distribution (spatial diversity).

The application of TR to communications where a sequence of data-modulated pulses is transmitted at a high rate relies totally on the behavior of the q-function. The condition of zero ISI

is to have a q-function that approaches a delta function, thus recovering the time reversed version of the original signal $s(-t)$ at the PS position. In practice, however, there always is some residual ISI because TR is optimized to maximize the SNR, rather than to eliminate the ISI, although the ISI can be reduced [e.g., see Fig. 5(b)] [9]. The extent of the ISI will affect the performance of time-reversal communications especially for higher order constellations unless the data rate is reduced to accommodate the ISI (rate backoff). Furthermore, a slight change in the environment over the two-way propagation interval introduces additional ISI. In this paper, we combine time-reversal communications with adaptive channel equalization to eliminate or minimize the residual ISI so that the performance of TR alone can be improved without sacrificing the data rate. In Section III, we investigate the performance of time-reversal communication with equalization.

III. TR COMMUNICATION WITH EQUALIZATION

In this section, we follow the derivations in [9] which provides analytical expressions for theoretical upper bounds on the performance of various approaches between a single element and a multielement array including TR. Here, we focus on the performance of TR with residual ISI and the performance of (active) TR with equalization and confirm that TR with equalization actually provides nearly optimal performance [11].

The overall system under consideration is illustrated in Fig. 1 where (active) TR is followed by a sampler operating at the symbol rate $1/T$ and a linear minimum mean square error (MSE) equalizer for estimating the information sequence from the sample values. Note that for the experimental results in Section IV, a fractionally spaced equalizer (FSE) is employed which samples the received signal at a higher rate as opposed to the symbol rate equalizer in this section.

We assume that the channel frequency responses $C_i(f), i = 1, \ldots, N$ are known for $|f| \leq W$ and that $C_i(f) = 0$ for $|f| > W$ where W is the channel bandwidth. The sequence of information symbols I_n is transmitted at a symbol rate $1/T$ and $w(t)$ represents the additive white Gaussian noise (AWGN)

with the power spectral density $S_w(f) = N_0$. The frequency responses of transmit and receive filters are $G_i(f)$ and $G_R(f)$, respectively. Let the overall (equivalent lowpass) channel transfer function be denoted by

$$F(f) = G_R(f) \sum_{i=1}^{N} G_i(f) C_i(f). \tag{2}$$

The received signal after filtering is then given by

$$y(t) = \sum_k I_k f(t - kT) + z(t) \tag{3}$$

and

$$S_z(f) = S_w(f) \left| G_R^2(f) \right|. \tag{4}$$

Note that $z(t)$ is the response of the receiving filter to the noise $w(t)$ with $\sigma_z^2 = \int_{-\infty}^{\infty} S_z(f) df$. If the transmitted energy per symbol is set to E and the sequence of information symbols is zero-mean and uncorrelated, the energy can be expressed as [12]

$$E = \sigma_I^2 \sum_{i=1}^{N} \int_{-\infty}^{\infty} \left| G_i^2(f) \right| df \tag{5}$$

where σ_I^2 denotes the variance of an information symbol.

A. Time-Reversal Performance With Residual ISI

When the received signal $y(t)$ is sampled at a rate of $1/T$, we have

$$y(nT) = I_n f(0) + \sum_{k \neq 0} I_{n-k} f(kT) + z(nT). \tag{6}$$

The output SNR is then given by

$$\mathrm{SNR}_{tr} = \frac{\sigma_I^2 |f^2(0)|}{\sigma_I^2 \sum_{k \neq 0} |f^2(kT)| + \sigma_z^2}. \tag{7}$$

For active (downlink) time-reversal communications, the transmitter filter uses $G_i(f) = K \sqrt{X(f)} C_i^*(f), i = 1, \ldots, N$ and the receive filter is simply $G_R(f) = \sqrt{X(f)}$ where K is a constant determined from the energy equation of (5). Note that $X(f)$ is equivalent to a probe pulse spectrum $X(f) = |S(f)|^2$ in TR which controls the system bandwidth. For simplicity, we consider the standard filter $X(f) = X_{rc}(f)$, i.e., a raised cosine filter with an arbitrary roll-off factor for zero ISI. Typically, it is split evenly between the transmitting and receiving filters as in [12] to distribute the computational complexity.

Then, the above output SNR can be expressed as in [9]

$$\mathrm{SNR}_{tr} = \frac{\dfrac{E}{N_0}}{\dfrac{E}{N_0} \rho + \dfrac{x(0)}{\int_{-\infty}^{\infty} X(f) \gamma(f) df}} \tag{8}$$

where

$$\rho = \frac{\sum_{k \neq 0} |f^2(kT)|}{|f^2(0)|} = \frac{T \int_{-1/2T}^{1/2T} |X\gamma[f]|^2 df}{\left| \int_{-\infty}^{\infty} X(f) \gamma(f) df \right|^2} - 1 \tag{9}$$

$$\gamma(f) = \sum_{i=1}^{N} |C_i^2(f)| \tag{10}$$

and $X\gamma[f]$ is the folded or aliased spectrum, where the folding frequency is $1/2T$ s

$$X\gamma[f] = \frac{1}{T} \sum_n X \left(f + \frac{n}{T} \right) \gamma \left(f + \frac{n}{T} \right) \tag{11}$$

where $\gamma(f)$ is the Fourier transform of the $q(t)$-function defined in (1). We observe that as the noise vanishes, i.e., $E/N_0 \to \infty$, the performance of TR saturates such that $\mathrm{SNR}_{tr} = 1/\rho$.

B. Time-Reversal Performance With Equalization

The performance of TR saturates due to residual ISI. A subsequent processing employed to overcome the limitation is an equalizer. Consider a sample-spaced linear equalizer that is optimized by using the minimum MSE (MMSE) criterion assuming that the equalizer has an infinite number of taps to derive a theoretical upper bound. For the received signal samples given in the form of (6), the MMSE equalizer has a transfer function [9], [12]

$$A[f] = \frac{\sigma_I^2 F^*[f]}{\sigma_I^2 |F[f]|^2 + S_z[f]} \tag{12}$$

where $F[f]$ is the folded spectrum of the overall response $F(f) = KX(f)\gamma(f)$ and $S_z[f] = N_0 X[f]$. Then, the minimum MSE can be expressed as

$$\mathrm{MMSE} = T \int_{-1/2T}^{1/2T} \frac{X[f]}{X[f] + \dfrac{\sigma_I^2}{N_0} |F[f]|^2} df. \tag{13}$$

Note that the above equation is different from [9, eq. (39)] where the equalizer is preceded by a receiver filter matched to the channel distorted transmitted pulse such that $G_R(f) = \sum_i G_i^*(f) C_i^*(f)$. The idea of active TR, however, is to apply matched filtering up front at the transmitter rather than at the receiver in passive TR while the two approaches without equalization provide the same performance [9]. Therefore, additional matched filtering is not required at the receiver and we use $G_R(f) = \sqrt{X(f)}$ resulting in the same overall channel response $F(f)$ as in Section III-A. It should be mentioned that the above equation is identical to [9, eq. (39)] when the roll-off factor of $X(f)$ is zero.

Then, the SNR at the equalizer output becomes

$$\mathrm{SNR}_{eq}$$
$$= \frac{1}{\mathrm{MMSE}} - 1$$
$$= \left[T \int_{-1/2T}^{1/2T} \frac{X[f]}{X[f] + \dfrac{E/N_0}{\int_{-\infty}^{\infty} X(f)\gamma(f) df} X^2 \gamma^2[f]} df \right]^{-1} - 1 \tag{14}$$

where $X^2 \gamma^2[f]$ is the folded spectrum of $X^2(f)\gamma^2(f)$.

C. Performance Improvement With Equalization: Numerical Example

Fig. 2 illustrates the performance improvement of TR with equalization over the case of TR alone. We use the same channel model in [9] with three multipaths (10-ms delay spread over a
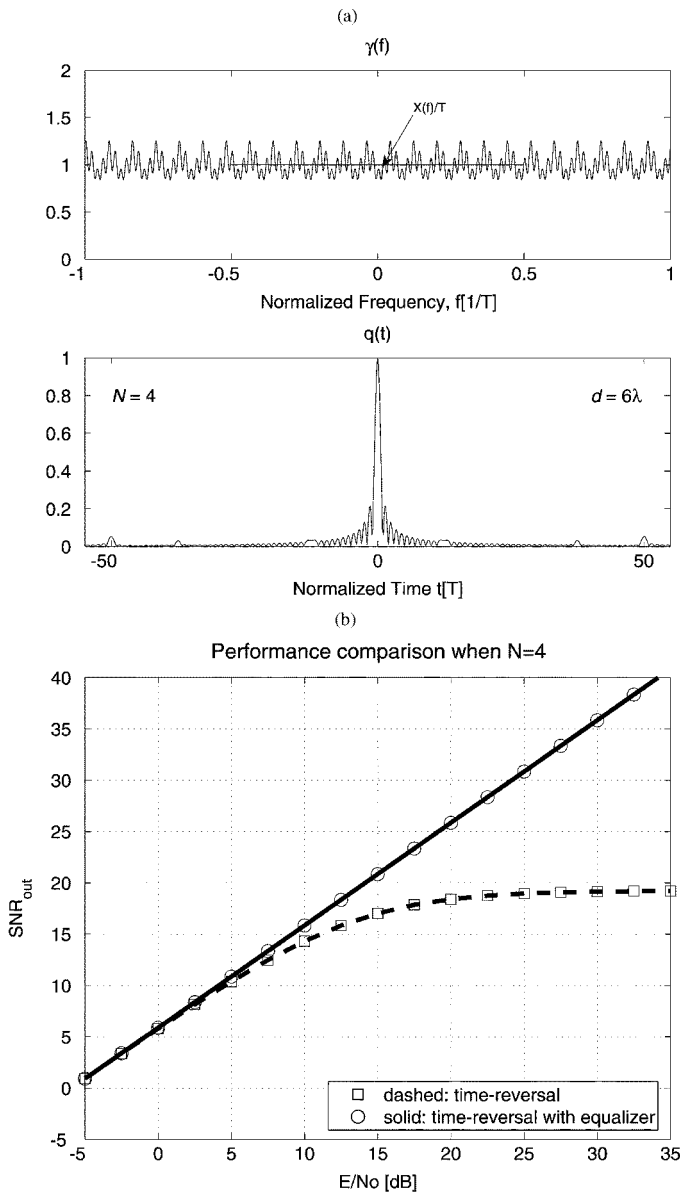
Fig. 2.   (a) Composite channel power spectral density $q(f)$, and the impulse response of TR, $q(t)$ function, when the number of array elements $N = 4$. The element spacing is chosen $d = 6\lambda_c$ with $\lambda_c = 0.1$ m at the center frequency $f_c = 15$ kHz. (b) Theoretical performance bounds: TR with residual ISI (square) and TR with equalization (circle).
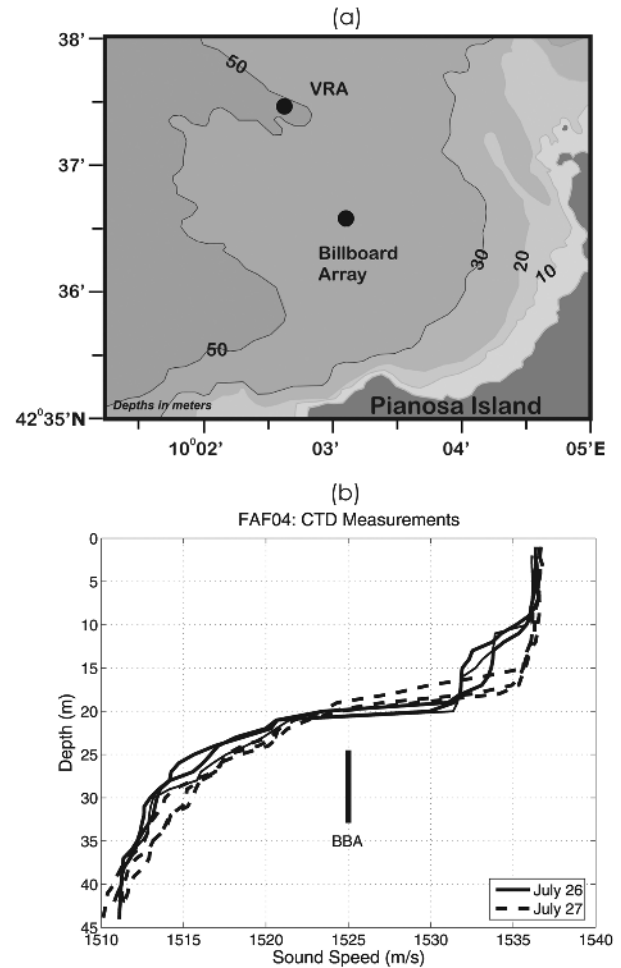

Fig. 3.   (a) Experimental area around Pianosa Island SW of Elba Island, off the west coast of Italy. The BBA was suspended from the R/V Alliance which was anchored in 50-m-deep water. The VRA was deployed at 2-km range from the BBA. (b) Sound-speed profile measured during the communications portion of the experiment on July 26 and 27, 2004 along with a depth coverage of the BBA.

3-km range) in 75-m-deep water. However, the element spacing of the vertical array is chosen $d = 6\lambda$, much larger than $d = \lambda/2$ which is typically used to avoid spatial aliasing in array processing. This is because the propagation angles are almost horizontal (broadside) in the acoustic waveguide (e.g., $\theta = 0°, 2.7°$, and $5.4°$). Further, 6λ is the element spacing of the time-reversal array used for the experimental results presented in Section IV.

The $q(t)$ function (bottom) and its spectrum $\gamma(f)$ (top) are shown in Fig. 2(a) when $N = 4$. As in [9], the standard filter $X(f)$ is chosen as a raised cosine with a roll-off factor close to 0, maximizing the data rate for ISI-free transmission in a bandwidth $W = 1/2T$. The symbol duration is then $T = 0.2$ ms with $2W = 5$ kHz and the center frequency is $f_c = 15$ kHz. It is interesting to observe that even with $N = 4$ elements $\gamma(f)$ flattens out and the overall system obtained with TR is almost

ideal. This results contrast with those in [9], where $N = 4$ element array with the interelement spacing of $d = \lambda/2$ at $f = 15$ kHz has an aperture of $L = 3\lambda/2$ which is not large enough to distinguish the three multipaths propagating closely at low grazing angles [11]. In fact, the minimum aperture L required for a one-sided resolution of $\Delta\theta = \lambda/2L = 2.7°$ near the broadside is $L \approx 10\lambda$. Note that the aperture of the $N = 4$ element array with 6λ spacing $(L = 18\lambda)$ is still 1.8 m in 75-m-deep water. Indeed, TR exploiting the spatial diversity is sensitive to the array size as pointed out in [9] as well as the spatial distribution of the array elements.

Fig. 2(b) shows the performance results when $N = 4$ [(8) and (14)]. As expected, the performance of TR with residual ISI (square) saturates with an increasing E/N_0 whereas the performance of TR with equalization (circle) continues to improve. At low and moderate E/N_0 up to about 7–8 dB, however, the two curves are almost identical suggesting that the time-reversal approach could be a choice with minimal computational complexity. This comes from the almost ideal behavior of the q-function in Fig. 2(a) which affects the point of separation between the two curves. For convenience, the q-function is normalized such that $q(0) = 1$ in Fig. 2(a) where $q(0)$ represents a total
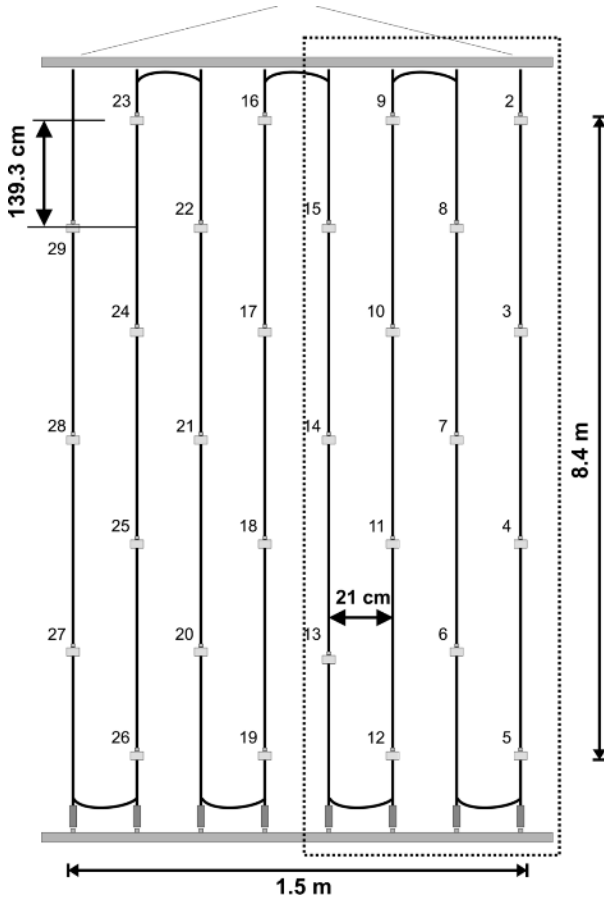
Fig. 4. Two-dimensional BBA reconfigured from a 78-m aperture time-reversal array with 2.786-m spacing. It consists of 28 elements on eight staves with 0.21-m spacing, spanning the water column from 24.5 to 32.9 m. During the communication experiment, only half of the array with 14 elements in the dashed box was used.

Fig. 5. (a) Example of the channel responses received by the BBA (Channels #2–15). (b) Corresponding $q(t)$ function.

energy of the channel impulse responses $c_i(t)$. However, this normalization should not be imposed when calculating the performance bounds as in [9], since we have a constraint on the transmitted energy E. This is important especially when the performance bounds are computed as a function of N, the number of array elements [11].

Although it is not shown here, the performance of TR with equalization is very close to the optimal processing proposed in [9]. The optimal processing was to simultaneously eliminate the ISI and maximize the SNR, while maintaining maximal data rate for a given bandwidth and satisfying a constraint on the transmitted energy. This suggests that we can relax the condition of zero ISI using TR at the front end while the overall system with equalization offers nearly optimal performance by removing the residual ISI. Therefore, we can take full advantage of the spatial focusing property of TR such that we can achieve a high SNR at the intended receiver along with low probability of interception elsewhere [e.g., see Fig. 9(a)]. This property allows an extension of TR to MIMO multiuser (active) communications with minimum interference between the users as demonstrated experimentally in [7]. Recently, it also has been shown in wireless communications based on outdoor measurements that the co-channel interference was reduced to about 18 dB [8].

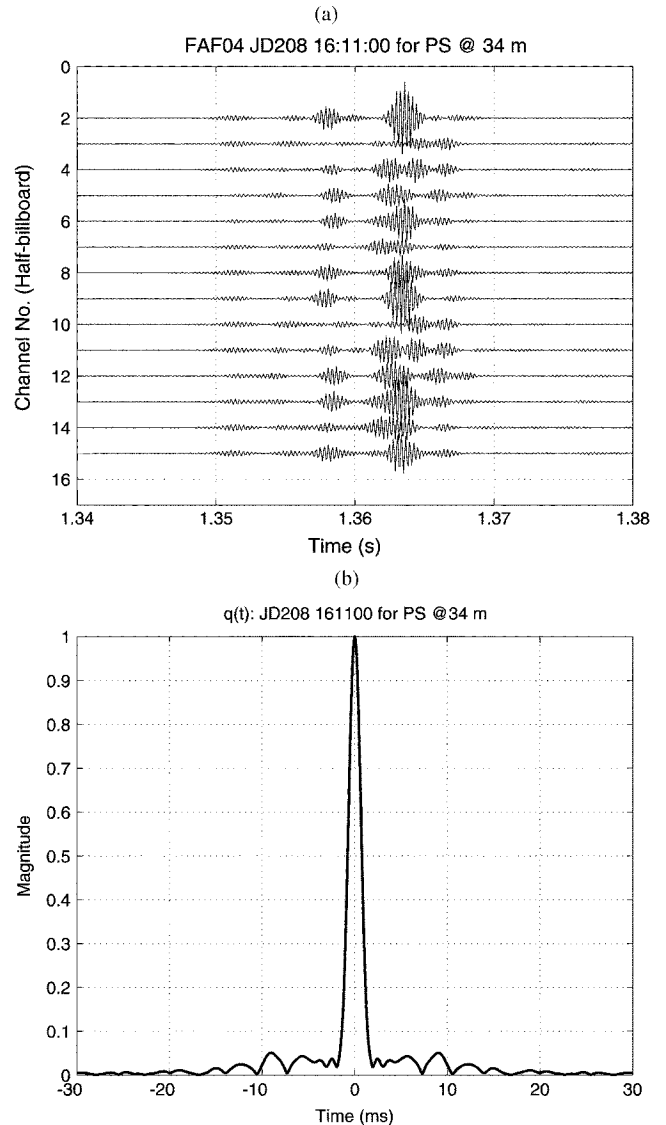For practical implementations, the benefit of this combination is that the number of taps required for an equalizer is much smaller than the case with just an equalizer alone, resulting in lower complexity at the equalizer. It should be pointed out that this approach does not require an explicit estimation of the channel impulse response $c_i(t)$. Instead, we use the captured channel response $s(t) * c_i(t)$ to generate a communication sequence for retransmission at the transmitter. In addition, carrier recovery for coherent communications can be done before the equalizer although there is some degradation effects due to residual ISI on the phase estimation [13], avoiding the complexity of the joint estimation of carrier phase and adaptive weight vectors within the equalizer (see Fig. 6). In Section IV, we demonstrate using experimental data in shallow water that TR combined with an adaptive channel equalizer indeed can improve the performance significantly.

IV. EXPERIMENTAL RESULTS

In this section, we present experimental results of time-reversal communications in conjunction with equalization between a time-reversal array and a single receiver separated 2 km
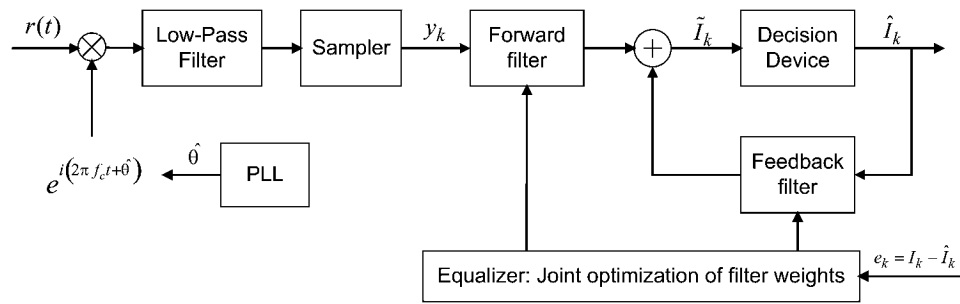
Fig. 6.   Block diagram showing time-reversal communications followed by a DFE equalizer. Note that a DFPLL has been applied before the equalizer.
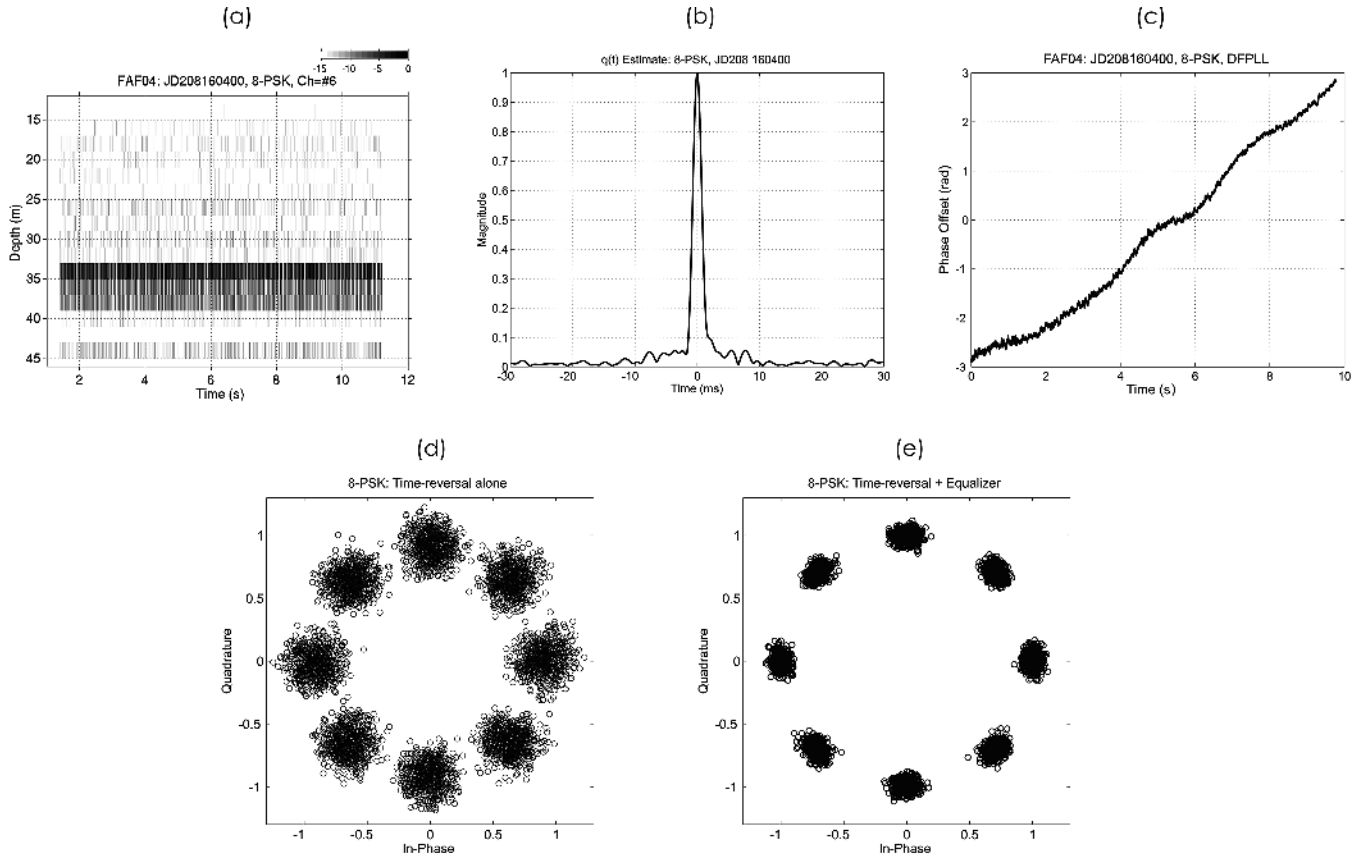

Fig. 7.   Performance of 8-PSK. (a) Time-reversal communications signal received on the VRA. The signal is focused on the intended receiver at 34-m depth (Element #6) of the VRA. The symbol SNR is 39 dB. (b) Estimated $q(t)$ function. (c) Phase tracking estimate using DFPLL. (d) Performance of the time-reversal processing alone. (e) Performance of TR in conjunction with an adaptive DFE.

in 50-m-deep water. We investigate three types of high-order phase coherent modulations suitable for a band-limited ocean environment: 8-PSK, 16-QAM, and 32-QAM. All communication sequences were 10-s long with the same symbol rate of $R = 1/T = 500$ symbols/s such that bit rates for 8-PSK, 16-QAM, and 32-QAM are $R_b = 1500, 2000,$ and 2500 bps, respectively. The carrier and sampling frequencies were $f_c = 3.5$ kHz with 1-kHz bandwidth and $f_s = 12$ kHz, respectively.

A. Experimental Setup: Billboard Array

A time-reversal experiment was conducted jointly with the NATO Undersea Research Center in July 2004 both north and south of Elba Island, off the west coast of Italy. The source/receive array (SRA) had 29 transducers spanning a 78-m aperture

with 2.786 m spacing which corresponds to about 6λ at 3.5 kHz [14]. The communication portion of the experiment reported in this paper was conducted at the Pianosa Island located south west of Elba as shown in Fig. 3 along with sound-speed profiles. The same SRA was reconfigured for deployment in 50-m-deep water for operation as a two-dimensional (2-D) billboard array (BBA) (8.4-m long and 1.5-m wide) as shown in Fig. 4. It consists of 28 elements distributed on eight staves with 0.21-m horizontal spacing between them which corresponds to a half-wavelength at 3.5 kHz. The BBA spanning the water column from 24.5 to 32.9 m was suspended from the R/V Alliance which was anchored for stable operation. A 16-element vertical receiver array (VRA) also was deployed about 2-km range from the BBA spanning the water column from 14 to 44 m with 2-m spacing. The purpose of the billboard array was to provide some
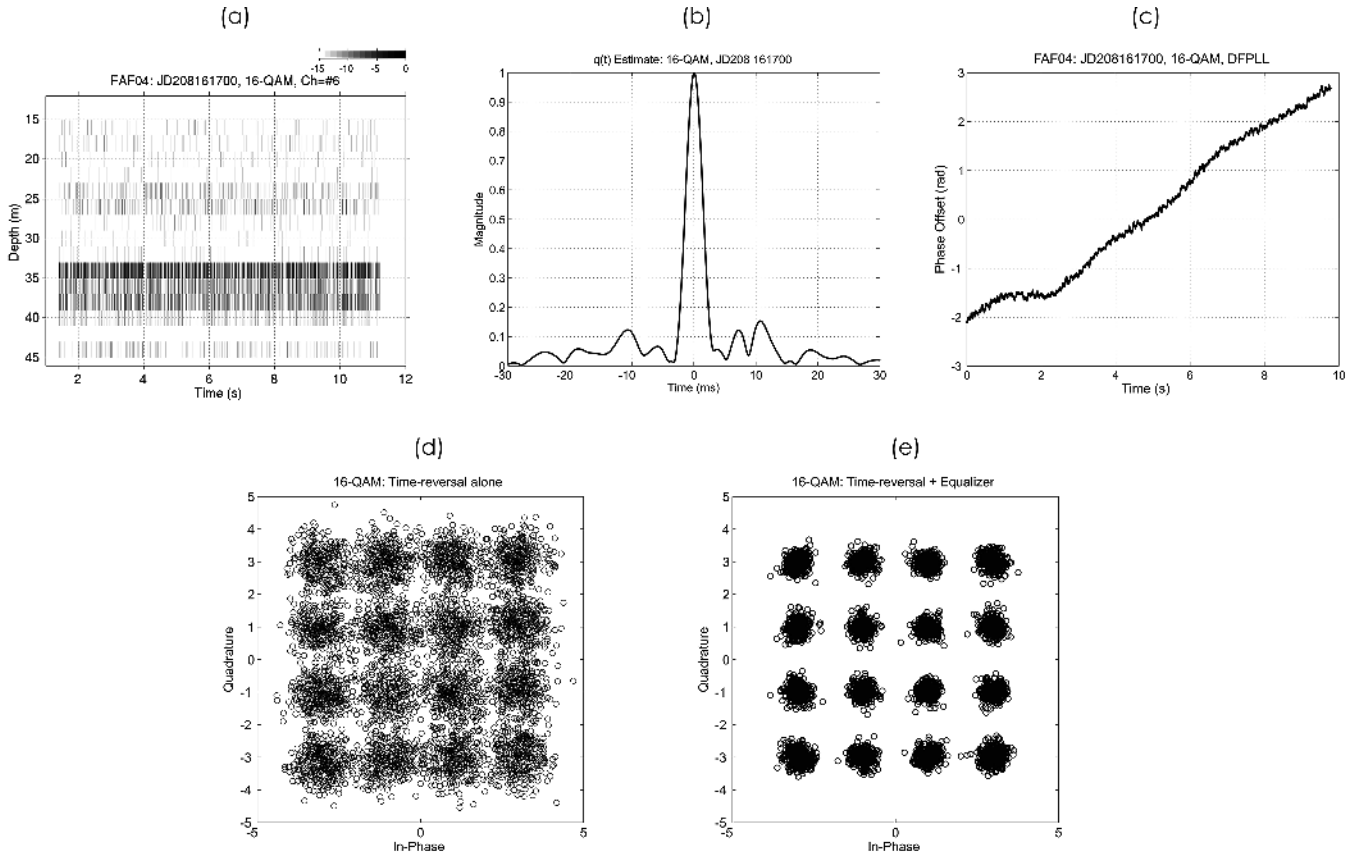
Fig. 8. Performance of 16-QAM. (a) Time-reversal communications signal received on the VRA. The signal is focused on the intended receiver at 34-m depth (Element #6) of the VRA. The symbol SNR is 34 dB. (b) Estimated $q(t)$ function. (c) Phase tracking estimate using DFPLL. (d) Performance of the time-reversal processing alone. (e) Performance of TR in conjunction with an adaptive DFE.

azimuthal (horizontal) discrimination in reverberation returns [15], but it also was used for the communications experiment. Note that only half of the array (i.e., 4 staves with $N = 14$ elements) as shown in Fig. 4 (dashed box) was actually used for the communications experiment reported in this paper.

B. Implementation: Time-Reversal Communication

There are two ways to implement time-reversal communications: conventional TR with a probe source (PS) and a MIMO approach without a probe source. The former has been used in our earlier experiments [15], [16] which requires a probe source collocated with the receiver array (VRA). The latter is a recent approach employed for MIMO communications [7] which can be implemented between an array of sources (SRA or BBA) and an array of receivers (VRA) without invoking reciprocity [17]. The process allows measurements of the channel transfer matrix between the two arrays almost instantly and the channel responses at the receiver array are transferred back to the source array to facilitate time-reversal communications. This implementation thus requires radio telemetry access to the receiver array data but does not require a PS to be collocated with the receiver array as in the conventional approach. These two implementations basically are equivalent and here we use the MIMO approach, although we communicate to a single receiver depth (user) on the VRA.

We used a 150-ms, 2.5–4.5-kHz chirp with a Hanning window for a probe signal $s(t)$, resulting in an effective 100-ms, 3–4-kHz bandwidth chirp [7]. An example of the channel responses is shown in Fig. 5 after compression (matched filtering) and the corresponding $q(t)$ function. Note that pairs of channels at the same depth (e.g., Channels 2 and 9, Channels 4 and 11) are very similar to each other. For time-reversal communications, the time reversed version of measured channel responses is treated as one symbol. Using the principle of superposition, each symbol is copied and displaced by the symbol interval $T = 2$ ms which is duration of the compressed chirp waveform. Although there is a substantial overlap of the transmitted symbols, the individual symbols are compressed back to their original $T = 2$-ms duration at the intended receiver.

C. Receiver Structure

It is shown in [7] that a simple receiver structure for time-reversal communication signals consists of a demodulator and detector, which is identical to the optimum receiver for signals corrupted by AWGN in the absence of ISI [12]. Here we cascade a nonlinear decision-feedback equalizer (DFE) to remove the residual ISI as shown in Fig. 6, where the filter weights (forward and feedback) are jointly optimized. The recursive least squares (RLS) algorithm has been used to adaptively perform this optimization. Since the symbol rate $1/T = 500$ Hz is only half
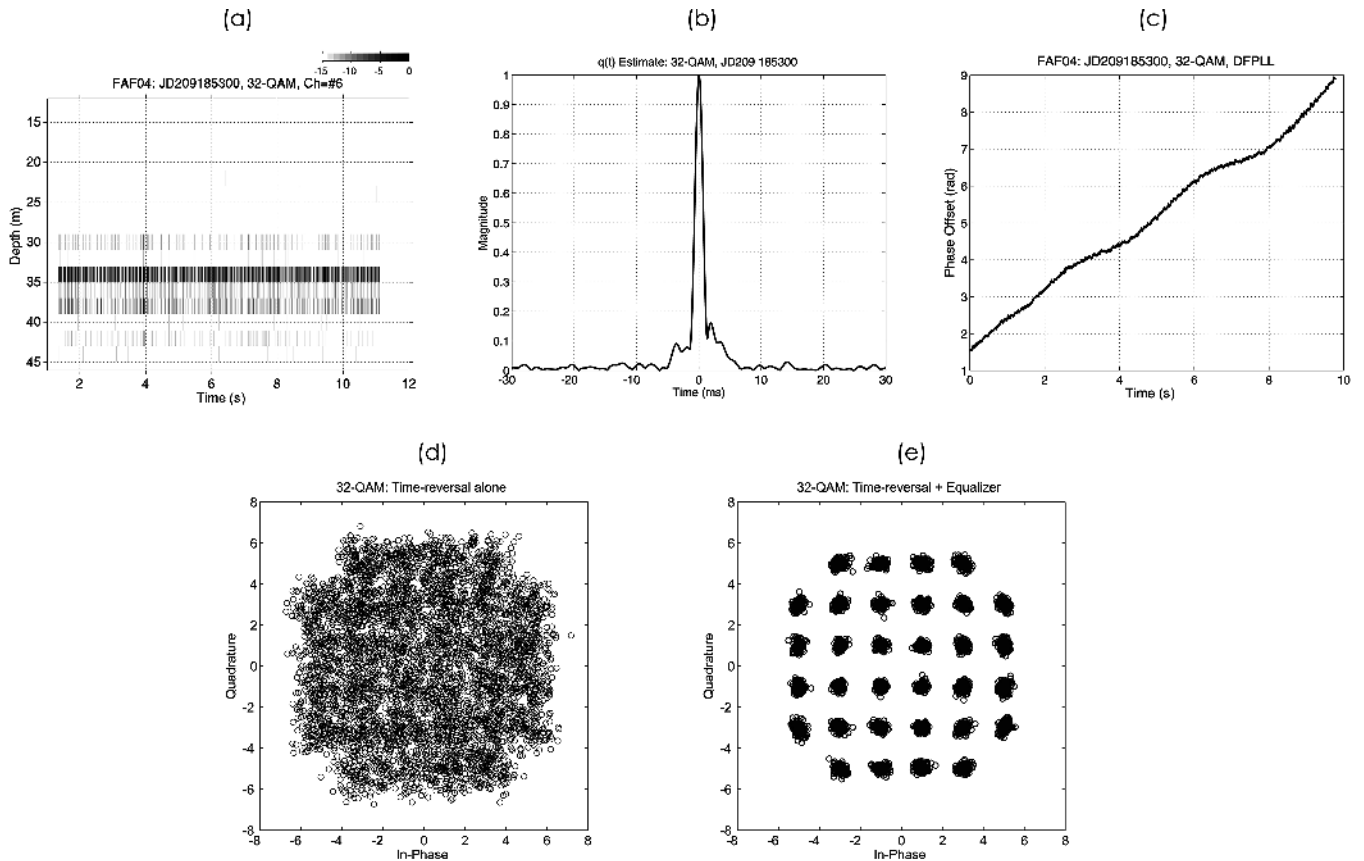
Fig. 9. Performance of 32-QAM. (a) Time-reversal communications signal received on the VRA. The signal is focused on the intended receiver at 34-m depth (Element #6) of the VRA. The symbol SNR is 44 dB. (b) Estimated $q(t)$ function. (c) Phase tracking estimate using DFPLL. (d) Performance of the time-reversal processing alone. (e) Performance of TR in conjunction with an adaptive DFE.

the signal bandwidth $2W = 1$ kHz of the chirp signal (equivalent to a raised cosine with a roll-off factor $\beta = 1$), we need to use a fractionally spaced equalizer (FSE) of at least $(1/2)T$ to avoid compensating for the aliased received signal. In this paper, we use $(1/4)T$ spaced equalizer which provides the best performance.

In our approach, the estimate of carrier phase is performed before the equalizer as indicated in Fig. 6. We employed the decision-feedback phase-locked loop (DFPLL) based on the maximum likelihood (ML) estimate averaged over 20 symbols [12]. We treat $\{I_n\}$ as a random sequence to be estimated except the first 100 or 200 training symbols which also are used in the adaptive DFE for channel estimation. Finally, the forgetting factor for RLS algorithm was set to 0.99.

D. Performance

Fig. 7 displays the result of 8-PSK modulation received at 34-m depth on the VRA (Element #6). The phase offset estimated by DFPLL is shown in Fig. 7(c). Note the average positive slope of about $\Delta\theta/\Delta t \approx 0.62$ rd/s which is equivalent to a frequency offset of 0.1 Hz. This was due to a slight difference in the sampling clocks between the BBA and VRA which varied from time to time.

The performance of time-reversal communication is shown in Fig. 7(d) resulting in a bit error rate (BER) of 4/14700 while the symbol SNR at the receiver was 39 dB. We expect a better

performance at this SNR but it appears that the residual ISI degraded the performance. To find out the extent of residual ISI, the q-function shown in Fig. 7(b) was estimated by correlating the received communication sequence with the entire known data sequence, essentially treating the data as a form of pseudorandom noise. The temporal sidelobes are not symmetric because the ocean changes over the two-way propagation interval (e.g., 3-min for this example). Fig. 7(e) shows an improved performance by cascading an adaptive DFE where the scattered symbols are tightened. The number of taps used for feedforward and backward DFE is $n_f = 20$ and $n_b = 2$, respectively. Recall that a $(1/4)T$ FSE is used for the feedforward filter. Then, $n_f = 20$ corresponds to five symbols (10 ms) which cover the most significant ISI around the peak shown in Fig. 7(b).

Now we look at the performance of 16-QAM modulation displayed in Fig. 8. The estimated q-function shows significant residual ISI compared to 8-PSK in Fig. 7(b). In addition, the nonsymmetrical nature of the ISI is more pronounced. The symbol SNR was 34 dB. The scatter plot with time-reversal processing in Fig. 8(d) yields 1% BER due to the significant ISI. Again, postprocessing using a FSE equalizer produces an open eye pattern with no errors in Fig. 8(e). The DFE used $n_f = 40$ and $n_b = 4$ taps with 200 training symbols.

Finally, the performance of 32-QAM modulation is shown in Fig. 9. The symbol SNR was 44 dB, but the performance of TR displayed in Fig. 9(d) clearly indicates the saturation effect due

to the residual ISI for this high-order constellation. The BER amounts to 5.4%. Fig. 9(e) highlights the performance improvement of TR combined with an adaptive DFE, showing a completely open eye pattern. The DFE used the same number of taps as used for 16-QAM above.

V. CONCLUSION

The spatial and temporal focusing properties of time-reversal methods offers a potential application to undersea communications with significant multipath. Spatial focusing mitigates the channel fading and produces a high SNR at the intended receivers along with a low probability of interception elsewhere. While temporal focusing (compression) reduces the ISI significantly, there always is some residual ISI. In addition, a slight change in the environment over the two-way propagation interval introduces additional ISI. Thus, the performance of time-reversal methods saturates due to the ISI. To avoid this limitation, we combine the time-reversal method with channel equalization, which theoretically provides nearly optimal performance as described in Section III-C.

During the July 2004 experiment, we investigated time-reversal communications at 2-km range in 50-m-deep water using a 14-element billboard array (8.4-m long and 0.6-m wide). The modulation schemes were coherent 8-PSK, 16-QAM, and 32-QAM. The symbol rate was 500 symbols/s at a carrier frequency of 3.5 kHz with a 1-kHz bandwidth and each communication sequence was 10 s long. Our analysis has demonstrated that the performance of time-reversal communication cascaded with adaptive DFEs can be improved significantly over the use of time-reversal processing alone.

REFERENCES

[1] D. Kilfoyle and A. Baggeroer, "The state of the art in underwater acoustic telemetry," *IEEE J. Ocean. Eng.*, vol. 25, no. 1, pp. 4–27, Jan. 2000.

[2] M. Stojanovic, J. Capitovic, and J. Proakis, "Adaptive multichannel combining and equalization for underwater acoustic communications," *J. Acoust. Soc. Amer.*, vol. 94, no. 3, pp. 1621–1631, Sep. 1993.

[3] W. A. Kuperman, W. S. Hodgkiss, H. C. Song, T. Akal, C. Ferla, and D. Jackson, "Phase conjugation in the ocean: Experimental demonstration of an acoustic time-reversal mirror," *J. Acoust. Soc. Amer.*, vol. 103, no. 1, pp. 25–40, Jan. 1998.

[4] M. Fink, "Time-reversed acoustics," *Sci. Amer.*, pp. 91–97, Nov. 1999.

[5] G. Edelmann, T. Akal, W. Hodgkiss, S. Kim, W. Kuperman, H. Song, and T. Akal, "An initial demonstration of underwater acoustic communication using time reversal mirror," *IEEE J. Ocean. Eng.*, vol. 27, no. 3, pp. 602–609, Jul. 2002.

[6] J. Flynn, J. Ritcey, D. Rouseff, and W. Fox, "Multichannel equalization by decision-directed passive phase conjugation: Experimental results," *IEEE J. Ocean. Eng.*, vol. 29, no. 3, pp. 824–836, Jul. 2004.

[7] H. Song, P. Roux, W. Hodgkiss, W. Kuperman, T. Akal, and M. Stevenson, "Multiple-input/multiple-output coherent time reversal communications in a shallow water acoustic channel," *IEEE J. Ocean. Eng.*, vol. 31, no. 1, pp. 170–178, Jan. 2006.

[8] H. Nguyen, J. Andersen, and G. Pederson, "The potential use of time reversal techniques in multiple element antenna systems," *IEEE Commun. Lett.*, vol. 9, no. 1, pp. 40–42, Jan. 2005.

[9] M. Stojanovic, "Retrofocusing techniques for high rate acoustic communications," *J. Acoust. Soc. Amer.*, vol. 117, no. 3, pp. 1173–1185, Mar 2005.

[10] T. Yang, "Temporal resolutions of time-reversed and passive-phase conjugation for underwater acoustic communication," *IEEE J. Ocean. Eng.*, vol. 28, no. 2, pp. 229–245, Apr. 2003.

[11] H. C. Song and A. Dotan, "Comments on "Retrofocusing techniques for high rate acoustic communication"[J. Acoust. Soc. Am., 117, 1173–1185] (L)," *J. Acoust. Soc. Amer.*, 2006, submitted for publication.

[12] J. Proakis, *Digital Communications.* New York: McGraw-Hill, 2001.

[13] S. Hinedi and W. Lindsey, "Intersymbol interference effects on bpsk and qpsk carrier tracking loops," *IEEE Trans. Commun.*, vol. 38, no. 10, pp. 1670–1676, Oct. 1990.

[14] W. S. Hodgkiss, J. D. Skinner, G. E. Edmonds, R. A. Harriss, and D. E. Ensberg, "A high frequency phase conjugation array," in *Proc. IEEE Oceans 2001*, 2001, pp. 1581–1585.

[15] H. C. Song, W. Hodgkiss, W. A. Kuperman, P. Roux, T. Akal, and M. Stevenson, "Experimental demonstration of adaptive reverberation nulling using time reversal mirror," *J. Acoust. Soc. Amer.*, vol. 118, no. 3, pp. 1381–1387, Sep. 2005.

[16] G. Edelmann, H. Song, S. Kim, W. Hodgkiss, W. Kuperman, and T. Akal, "Underwater acoustic communication using time reversal," *IEEE J. Ocean. Eng.*, vol. 30, no. 4, pp. 852–864, Oct. 2005.

[17] P. Roux, W. Kuperman, W. Hodgkiss, H. Song, T. Akal, and M. Stevenson, "A nonreciprocal implementations of time reversal in the ocean," *J. Acoust. Soc. Amer.*, vol. 116, pp. 1009–1015, Jun. 2004.

H. C. Song received the B.S. and M.S. degrees in marine engineering and naval architecture from Seoul National University, Korea, in 1978 and 1980, respectively, and the Ph.D. degree in ocean engineering from the Massachusetts Institute of Technology, Cambridge, in 1990.

From 1991 to 1995, he was with Korea Ocean Research and Development Institute. Since 1996, he has been a member of the scientists of the Marine Physical Laboratory/Scripps Institution of Oceanography, University of California, San Diego. His research interests include time-reversed acoustics, robust matched field processing, and underwater communications.

Dr. Song is a Fellow of the Acoustical Society of America.

W. S. Hodgkiss (S'68–M'75) was born in Bellefonte, PA, on August 20, 1950. He received the B.S.E.E. degree from Bucknell University, Lewisburg, PA, in 1972, and the M.S. and Ph.D. degrees in electrical engineering from Duke University, Durham, NC, in 1973 and 1975, respectively.

From 1975 to 1977, he worked with the Naval Ocean Systems Center, San Diego, CA. From 1977 to 1978, he was a faculty member in the Electrical Engineering Department, Bucknell University. Since 1978, he has been a member of the faculty of the Scripps Institution of Oceanography, University of California, San Diego, and on the staff of the Marine Physical Laboratory. Currently, he is the Deputy Director, Scientific Affairs, Scripps Institution of Oceanography. His present research interests are in the areas of signal processing, propagation modeling, and environmental inversions with applications of these to underwater acoustics and electromagnetic wave propagation.

Dr. Hodgkiss is a Fellow of the Acoustical Society of America.

W. A. Kuperman has worked at the Naval Research Laboratory, the SACLANT Undersea Research Centre in La Spezia, Italy, and most recently, at the Scripps Institution of Oceanography of the University of California, San Diego, where he is a Professor and Director of its Marine Physical Laboratory. He has done theoretical and experimental research in ocean acoustics and signal processing.

M. Stevenson received the degree from the U.S. Naval Academy and Scripps Institution of Oceanography, University of California, San Diego.

He joined the Acoustic Branch of the Space and Naval Warfare Systems Center. His past research includes design and deployment of acoustic measurement arrays under the Arctic icecap and in coastal, shallow-water environments. He is presently the project leader for focused acoustic field studies at the NATO Undersea Research Centre, La Spezia, Italy.

T. Akal was a Principal Senior Scientist at SACLANT Undersea Research Center, La Spezia, Italy, where, over the past 33 years, he has been leading research projects related to underwater acoustic and seismic propagation and marine sediment acoustics. Now he is collaborating with TUBITAK–Marmara Research Center, Earth and Marine Sciences Research Institute in Turkey, Marine Physical Laboratory of Scripps Institution of Oceanography at University of California, San Diego, and Lamont–Doherty Earth Observatory of Columbia University Palisades, New York.